

Angular distributions in the decay $B \rightarrow K^* l^+ l^-$

B. Aubert,¹ M. Bona,¹ Y. Karyotakis,¹ J. P. Lees,¹ V. Poireau,¹ X. Prudent,¹ V. Tisserand,¹ A. Zghiche,¹ J. Garra Tico,² E. Grauges,² L. Lopez,³ A. Palano,³ M. Pappagallo,³ G. Eigen,⁴ B. Stugu,⁴ L. Sun,⁴ G. S. Abrams,⁵ M. Battaglia,⁵ D. N. Brown,⁵ J. Button-Shafer,⁵ R. N. Cahn,⁵ R. G. Jacobsen,⁵ J. A. Kadyk,⁵ L. T. Kerth,⁵ Yu. G. Kolomensky,⁵ G. Kukartsev,⁵ G. Lynch,⁵ I. L. Osipenkov,⁵ M. T. Ronan,^{5,*} K. Tackmann,⁵ T. Tanabe,⁵ W. A. Wenzel,⁵ C. M. Hawkes,⁶ N. Soni,⁶ A. T. Watson,⁶ H. Koch,⁷ T. Schroeder,⁷ D. Walker,⁸ D. J. Asgeirsson,⁹ T. Cuhadar-Donszelmann,⁹ B. G. Fulsom,⁹ C. Hearty,⁹ T. S. Mattison,⁹ J. A. McKenna,⁹ M. Barrett,¹⁰ A. Khan,¹⁰ M. Saleem,¹⁰ L. Teodorescu,¹⁰ V. E. Blinov,¹¹ A. D. Bukin,¹¹ A. R. Buzykaev,¹¹ V. P. Druzhinin,¹¹ V. B. Golubev,¹¹ A. P. Onuchin,¹¹ S. I. Serednyakov,¹¹ Yu. I. Skovpen,¹¹ E. P. Solodov,¹¹ K. Yu. Todyshev,¹¹ M. Bondioli,¹² S. Curry,¹² I. Eschrich,¹² D. Kirkby,¹² A. J. Lankford,¹² P. Lund,¹² M. Mandelkern,¹² E. C. Martin,¹² D. P. Stoker,¹² S. Abachi,¹³ C. Buchanan,¹³ J. W. Gary,¹⁴ F. Liu,¹⁴ O. Long,¹⁴ B. C. Shen,^{14,*} G. M. Vitug,¹⁴ Z. Yasin,¹⁴ L. Zhang,¹⁴ V. Sharma,¹⁵ C. Campagnari,¹⁶ T. M. Hong,¹⁶ D. Kovalskiy,¹⁶ M. A. Mazur,¹⁶ J. D. Richman,¹⁶ T. W. Beck,¹⁷ A. M. Eisner,¹⁷ C. J. Flacco,¹⁷ C. A. Heusch,¹⁷ J. Kroseberg,¹⁷ W. S. Lockman,¹⁷ T. Schalk,¹⁷ B. A. Schumm,¹⁷ A. Seiden,¹⁷ L. Wang,¹⁷ M. G. Wilson,¹⁷ L. O. Winstrom,¹⁷ C. H. Cheng,¹⁸ D. A. Doll,¹⁸ B. Echenard,¹⁸ F. Fang,¹⁸ D. G. Hitlin,¹⁸ I. Narsky,¹⁸ T. Piatenko,¹⁸ F. C. Porter,¹⁸ R. Andreassen,¹⁹ G. Mancinelli,¹⁹ B. T. Meadows,¹⁹ K. Mishra,¹⁹ M. D. Sokoloff,¹⁹ F. Blanc,²⁰ P. C. Bloom,²⁰ W. T. Ford,²⁰ J. F. Hirschauer,²⁰ A. Kreisel,²⁰ M. Nagel,²⁰ U. Nauenberg,²⁰ A. Olivas,²⁰ J. G. Smith,²⁰ K. A. Ulmer,²⁰ S. R. Wagner,²⁰ R. Ayad,^{21,†} A. M. Gabareen,²¹ A. Soffer,^{21,‡} W. H. Toki,²¹ R. J. Wilson,²¹ D. D. Altenburg,²² E. Feltresi,²² A. Hauke,²² H. Jasper,²² M. Karbach,²² J. Merkel,²² A. Petzold,²² B. Spaan,²² K. Wacker,²² V. Klose,²³ M. J. Kobel,²³ H. M. Lacker,²³ W. F. Mader,²³ R. Nogowski,²³ J. Schubert,²³ K. R. Schubert,²³ R. Schwierz,²³ J. E. Sundermann,²³ A. Volk,²³ D. Bernard,²⁴ G. R. Bonneaud,²⁴ E. Latour,²⁴ Ch. Thiebaux,²⁴ M. Verderi,²⁴ P. J. Clark,²⁵ W. Gradl,²⁵ S. Playfer,²⁵ A. I. Robertson,²⁵ J. E. Watson,²⁵ M. Andreotti,²⁶ D. Bettoni,²⁶ C. Bozzi,²⁶ R. Calabrese,²⁶ A. Cecchi,²⁶ G. Cibinetto,²⁶ P. Franchini,²⁶ E. Luppi,²⁶ M. Negrini,²⁶ A. Petrella,²⁶ L. Piemontese,²⁶ E. Prencipe,²⁶ V. Santoro,²⁶ F. Anulli,²⁷ R. Baldini-Ferrolli,²⁷ A. Calcaterra,²⁷ R. de Sangro,²⁷ G. Finocchiaro,²⁷ S. Pacetti,²⁷ P. Patteri,²⁷ I. M. Peruzzi,^{27,§} M. Piccolo,²⁷ M. Rama,²⁷ A. Zallo,²⁷ A. Buzzo,²⁸ R. Contri,²⁸ M. Lo Vetere,²⁸ M. M. Macri,²⁸ M. R. Monge,²⁸ S. Passaggio,²⁸ C. Patrignani,²⁸ E. Robutti,²⁸ A. Santroni,²⁸ S. Tosi,²⁸ K. S. Chaisanguanthum,²⁹ M. Morii,²⁹ R. S. Dubitzky,³⁰ J. Marks,³⁰ S. Schenk,³⁰ U. Uwer,³⁰ D. J. Bard,³¹ P. D. Dauncey,³¹ J. A. Nash,³¹ W. Panduro Vazquez,³¹ M. Tibbetts,³¹ P. K. Behera,³² X. Chai,³² M. J. Charles,³² U. Mallik,³² J. Cochran,³³ H. B. Crawley,³³ L. Dong,³³ W. T. Meyer,³³ S. Prell,³³ E. I. Rosenberg,³³ A. E. Rubin,³³ Y. Y. Gao,³⁴ A. V. Gritsan,³⁴ Z. J. Guo,³⁴ C. K. Lae,³⁴ A. G. Denig,³⁵ M. Fritsch,³⁵ G. Schott,³⁵ N. Arnaud,³⁶ J. Béquilleux,³⁶ A. D'Orazio,³⁶ M. Davier,³⁶ J. Firmino da Costa,³⁶ G. Grosdidier,³⁶ A. Höcker,³⁶ V. Lepeltier,³⁶ F. Le Diberder,³⁶ A. M. Lutz,³⁶ S. Pruvot,³⁶ P. Roudeau,³⁶ M. H. Schune,³⁶ J. Serrano,³⁶ V. Sordini,³⁶ A. Stocchi,³⁶ W. F. Wang,³⁶ G. Wormser,³⁶ D. J. Lange,³⁷ D. M. Wright,³⁷ I. Bingham,³⁸ J. P. Burke,³⁸ C. A. Chavez,³⁸ J. R. Fry,³⁸ E. Gabathuler,³⁸ R. Gamet,³⁸ D. E. Hutchcroft,³⁸ D. J. Payne,³⁸ C. Touramanis,³⁸ A. J. Bevan,³⁹ K. A. George,³⁹ F. Di Lodovico,³⁹ R. Sacco,³⁹ M. Sigamani,³⁹ G. Cowan,⁴⁰ H. U. Flaecher,⁴⁰ D. A. Hopkins,⁴⁰ S. Paramesvaran,⁴⁰ F. Salvatore,⁴⁰ A. C. Wren,⁴⁰ D. N. Brown,⁴¹ C. L. Davis,⁴¹ K. E. Alwyn,⁴² N. R. Barlow,⁴² R. J. Barlow,⁴² Y. M. Chia,⁴² C. L. Edgar,⁴² G. D. Lafferty,⁴² T. J. West,⁴² J. I. Yi,⁴² J. Anderson,⁴³ C. Chen,⁴³ A. Jawahery,⁴³ D. A. Roberts,⁴³ G. Simi,⁴³ J. M. Tuggle,⁴³ C. Dallapiccola,⁴⁴ S. S. Hertzbach,⁴⁴ X. Li,⁴⁴ E. Salvati,⁴⁴ S. Saremi,⁴⁴ R. Cowan,⁴⁵ D. Dujmic,⁴⁵ P. H. Fisher,⁴⁵ K. Koeneke,⁴⁵ G. Sciolla,⁴⁵ M. Spitznagel,⁴⁵ F. Taylor,⁴⁵ R. K. Yamamoto,⁴⁵ M. Zhao,⁴⁵ S. E. Mclachlin,^{46,*} P. M. Patel,⁴⁶ S. H. Robertson,⁴⁶ A. Lazzaro,⁴⁷ V. Lombardo,⁴⁷ F. Palombo,⁴⁷ J. M. Bauer,⁴⁸ L. Cremaldi,⁴⁸ V. Eschenburg,⁴⁸ R. Godang,⁴⁸ R. Kroeger,⁴⁸ D. A. Sanders,⁴⁸ D. J. Summers,⁴⁸ H. W. Zhao,⁴⁸ S. Brunet,⁴⁹ D. Côté,⁴⁹ M. Simard,⁴⁹ P. Taras,⁴⁹ F. B. Viaud,⁴⁹ H. Nicholson,⁵⁰ G. De Nardo,⁵¹ L. Lista,⁵¹ D. Monorchio,⁵¹ C. Sciacca,⁵¹ M. A. Baak,⁵² G. Raven,⁵² H. L. Snoek,⁵² C. P. Jessop,⁵³ K. J. Knoepfel,⁵³ J. M. LoSecco,⁵³ G. Benelli,⁵⁴ L. A. Corwin,⁵⁴ K. Honscheid,⁵⁴ H. Kagan,⁵⁴ R. Kass,⁵⁴ J. P. Morris,⁵⁴ A. M. Rahimi,⁵⁴ J. J. Regensburger,⁵⁴ S. J. Sekula,⁵⁴ Q. K. Wong,⁵⁴ N. L. Blount,⁵⁵ J. Brau,⁵⁵ R. Frey,⁵⁵ O. Igonkina,⁵⁵ J. A. Kolb,⁵⁵ M. Lu,⁵⁵ R. Rahmat,⁵⁵ N. B. Sinev,⁵⁵ D. Strom,⁵⁵ J. Strube,⁵⁵ E. Torrence,⁵⁵ G. Castelli,⁵⁶ N. Gagliardi,⁵⁶ A. Gaz,⁵⁶ M. Margoni,⁵⁶ M. Morandin,⁵⁶ M. Posocco,⁵⁶ M. Rotondo,⁵⁶ F. Simonetto,⁵⁶ R. Stroili,⁵⁶ C. Voci,⁵⁶ P. del Amo Sanchez,⁵⁷ E. Ben-Haim,⁵⁷ H. Briand,⁵⁷ G. Calderini,⁵⁷ J. Chauveau,⁵⁷ P. David,⁵⁷ L. Del Buono,⁵⁷ O. Hamon,⁵⁷ Ph. Leruste,⁵⁷ J. Ocariz,⁵⁷ A. Perez,⁵⁷ J. Prendki,⁵⁷ L. Gladney,⁵⁸ M. Biasini,⁵⁹ R. Covarelli,⁵⁹ E. Manoni,⁵⁹ C. Angelini,⁶⁰ G. Batignani,⁶⁰ S. Bettarini,⁶⁰ M. Carpinelli,^{60,||} A. Cervelli,⁶⁰ F. Forti,⁶⁰ M. A. Giorgi,⁶⁰ A. Lusiani,⁶⁰ G. Marchiori,⁶⁰ M. Morganti,⁶⁰ N. Neri,⁶⁰ E. Paoloni,⁶⁰ G. Rizzo,⁶⁰ J. J. Walsh,⁶⁰ J. Biesiada,⁶¹ Y. P. Lau,⁶¹ D. Lopes Pegna,⁶¹ C. Lu,⁶¹ J. Olsen,⁶¹ A. J. S. Smith,⁶¹ A. V. Telnov,⁶¹ E. Baracchini,⁶²

G. Cavoto,⁶² D. del Re,⁶² E. Di Marco,⁶² R. Faccini,⁶² F. Ferrarotto,⁶² F. Ferroni,⁶² M. Gaspero,⁶² P. D. Jackson,⁶² L. Li Gioi,⁶² M. A. Mazzoni,⁶² S. Morganti,⁶² G. Piredda,⁶² F. Polci,⁶² F. Renga,⁶² C. Voena,⁶² M. Ebert,⁶³ T. Hartmann,⁶³ H. Schröder,⁶³ R. Waldi,⁶³ T. Adye,⁶⁴ B. Franek,⁶⁴ E. O. Olaiya,⁶⁴ W. Roethel,⁶⁴ F. F. Wilson,⁶⁴ S. Emery,⁶⁵ M. Escalier,⁶⁵ L. Esteve,⁶⁵ A. Gaidot,⁶⁵ S. F. Ganzhur,⁶⁵ G. Hamel de Monchenault,⁶⁵ W. Kozanecki,⁶⁵ G. Vasseur,⁶⁵ Ch. Yèche,⁶⁵ M. Zito,⁶⁵ X. R. Chen,⁶⁶ H. Liu,⁶⁶ W. Park,⁶⁶ M. V. Purohit,⁶⁶ R. M. White,⁶⁶ J. R. Wilson,⁶⁶ M. T. Allen,⁶⁷ D. Aston,⁶⁷ R. Bartoldus,⁶⁷ P. Bechtle,⁶⁷ J. F. Benitez,⁶⁷ R. Cenci,⁶⁷ J. P. Coleman,⁶⁷ M. R. Convery,⁶⁷ J. C. Dingfelder,⁶⁷ J. Dorfan,⁶⁷ G. P. Dubois-Felsmann,⁶⁷ W. Dunwoodie,⁶⁷ R. C. Field,⁶⁷ S. J. Gowdy,⁶⁷ M. T. Graham,⁶⁷ P. Grenier,⁶⁷ C. Hast,⁶⁷ W. R. Innes,⁶⁷ J. Kaminski,⁶⁷ M. H. Kelsey,⁶⁷ H. Kim,⁶⁷ P. Kim,⁶⁷ M. L. Kocian,⁶⁷ D. W. G. S. Leith,⁶⁷ S. Li,⁶⁷ B. Lindquist,⁶⁷ S. Luitz,⁶⁷ V. Luth,⁶⁷ H. L. Lynch,⁶⁷ D. B. MacFarlane,⁶⁷ H. Marsiske,⁶⁷ R. Messner,⁶⁷ D. R. Muller,⁶⁷ H. Neal,⁶⁷ S. Nelson,⁶⁷ C. P. O'Grady,⁶⁷ I. Ofte,⁶⁷ A. Perazzo,⁶⁷ M. Perl,⁶⁷ B. N. Ratcliff,⁶⁷ A. Roodman,⁶⁷ A. A. Salnikov,⁶⁷ R. H. Schindler,⁶⁷ J. Schwiening,⁶⁷ A. Snyder,⁶⁷ D. Su,⁶⁷ M. K. Sullivan,⁶⁷ K. Suzuki,⁶⁷ S. K. Swain,⁶⁷ J. M. Thompson,⁶⁷ J. Va'vra,⁶⁷ A. P. Wagner,⁶⁷ M. Weaver,⁶⁷ C. A. West,⁶⁷ W. J. Wisniewski,⁶⁷ M. Wittgen,⁶⁷ D. H. Wright,⁶⁷ H. W. Wulsin,⁶⁷ A. K. Yarritu,⁶⁷ K. Yi,⁶⁷ C. C. Young,⁶⁷ V. Ziegler,⁶⁷ P. R. Burchat,⁶⁸ A. J. Edwards,⁶⁸ S. A. Majewski,⁶⁸ T. S. Miyashita,⁶⁸ B. A. Petersen,⁶⁸ L. Wilden,⁶⁸ S. Ahmed,⁶⁹ M. S. Alam,⁶⁹ R. Bula,⁶⁹ J. A. Ernst,⁶⁹ B. Pan,⁶⁹ M. A. Saeed,⁶⁹ S. B. Zain,⁶⁹ S. M. Spanier,⁷⁰ B. J. Wogslund,⁷⁰ R. Eckmann,⁷¹ J. L. Ritchie,⁷¹ A. M. Ruland,⁷¹ C. J. Schilling,⁷¹ R. F. Schwitters,⁷¹ B. W. Drummond,⁷² J. M. Izen,⁷² X. C. Lou,⁷² S. Ye,⁷² F. Bianchi,⁷³ D. Gamba,⁷³ M. Pelliccioni,⁷³ M. Bomben,⁷⁴ L. Bosisio,⁷⁴ C. Cartaro,⁷⁴ G. Della Ricca,⁷⁴ L. Lanceri,⁷⁴ L. Vitale,⁷⁴ V. Azzolini,⁷⁵ N. Lopez-March,⁷⁵ F. Martinez-Vidal,⁷⁵ D. A. Milanes,⁷⁵ A. Oyanguren,⁷⁵ J. Albert,⁷⁶ Sw. Banerjee,⁷⁶ B. Bhuyan,⁷⁶ H. H. F. Choi,⁷⁶ K. Hamano,⁷⁶ R. Kowalewski,⁷⁶ M. J. Lewczuk,⁷⁶ I. M. Nugent,⁷⁶ J. M. Roney,⁷⁶ R. J. Sobie,⁷⁶ T. J. Gershon,⁷⁷ P. F. Harrison,⁷⁷ J. Ilic,⁷⁷ T. E. Latham,⁷⁷ G. B. Mohanty,⁷⁷ H. R. Band,⁷⁸ X. Chen,⁷⁸ S. Dasu,⁷⁸ K. T. Flood,⁷⁸ Y. Pan,⁷⁸ M. Pierini,⁷⁸ R. Prepost,⁷⁸ C. O. Vuosalo,⁷⁸ and S. L. Wu⁷⁸

(BABAR Collaboration)

¹Laboratoire de Physique des Particules, IN2P3/CNRS et Université de Savoie, F-74941 Annecy-Le-Vieux, France

²Universitat de Barcelona, Facultat de Física, Departament ECM, E-08028 Barcelona, Spain

³Università di Bari, Dipartimento di Fisica and INFN, I-70126 Bari, Italy

⁴University of Bergen, Institute of Physics, N-5007 Bergen, Norway

⁵Lawrence Berkeley National Laboratory and University of California, Berkeley, California 94720, USA

⁶University of Birmingham, Birmingham, B15 2TT, United Kingdom

⁷Ruhr Universität Bochum, Institut für Experimentalphysik I, D-44780 Bochum, Germany

⁸University of Bristol, Bristol BS8 1TL, United Kingdom

⁹University of British Columbia, Vancouver, British Columbia, Canada V6T 1Z1

¹⁰Brunel University, Uxbridge, Middlesex UB8 3PH, United Kingdom

¹¹Budker Institute of Nuclear Physics, Novosibirsk 630090, Russia

¹²University of California at Irvine, Irvine, California 92697, USA

¹³University of California at Los Angeles, Los Angeles, California 90024, USA

¹⁴University of California at Riverside, Riverside, California 92521, USA

¹⁵University of California at San Diego, La Jolla, California 92093, USA

¹⁶University of California at Santa Barbara, Santa Barbara, California 93106, USA

¹⁷University of California at Santa Cruz, Institute for Particle Physics, Santa Cruz, California 95064, USA

¹⁸California Institute of Technology, Pasadena, California 91125, USA

¹⁹University of Cincinnati, Cincinnati, Ohio 45221, USA

²⁰University of Colorado, Boulder, Colorado 80309, USA

²¹Colorado State University, Fort Collins, Colorado 80523, USA

²²Universität Dortmund, Institut für Physik, D-44221 Dortmund, Germany

²³Technische Universität Dresden, Institut für Kern- und Teilchenphysik, D-01062 Dresden, Germany

²⁴Laboratoire Leprince-Ringuet, CNRS/IN2P3, Ecole Polytechnique, F-91128 Palaiseau, France

²⁵University of Edinburgh, Edinburgh EH9 3JZ, United Kingdom

²⁶Università di Ferrara, Dipartimento di Fisica and INFN, I-44100 Ferrara, Italy

²⁷Laboratori Nazionali di Frascati dell'INFN, I-00044 Frascati, Italy

²⁸Università di Genova, Dipartimento di Fisica and INFN, I-16146 Genova, Italy

²⁹Harvard University, Cambridge, Massachusetts 02138, USA

³⁰Universität Heidelberg, Physikalisches Institut, Philosophenweg 12, D-69120 Heidelberg, Germany

³¹Imperial College London, London, SW7 2AZ, United Kingdom

³²University of Iowa, Iowa City, Iowa 52242, USA

³³Iowa State University, Ames, Iowa 50011-3160, USA

³⁴Johns Hopkins University, Baltimore, Maryland 21218, USA

- ³⁵Universität Karlsruhe, Institut für Experimentelle Kernphysik, D-76021 Karlsruhe, Germany
- ³⁶Laboratoire de l'Accélérateur Linéaire, IN2P3/CNRS et Université Paris-Sud 11, Centre Scientifique d'Orsay, B. P. 34, F-91898 ORSAY Cedex, France
- ³⁷Lawrence Livermore National Laboratory, Livermore, California 94550, USA
- ³⁸University of Liverpool, Liverpool L69 7ZE, United Kingdom
- ³⁹Queen Mary, University of London, E1 4NS, United Kingdom
- ⁴⁰University of London, Royal Holloway and Bedford New College, Egham, Surrey TW20 0EX, United Kingdom
- ⁴¹University of Louisville, Louisville, Kentucky 40292, USA
- ⁴²University of Manchester, Manchester M13 9PL, United Kingdom
- ⁴³University of Maryland, College Park, Maryland 20742, USA
- ⁴⁴University of Massachusetts, Amherst, Massachusetts 01003, USA
- ⁴⁵Massachusetts Institute of Technology, Laboratory for Nuclear Science, Cambridge, Massachusetts 02139, USA
- ⁴⁶McGill University, Montréal, Québec, Canada H3A 2T8
- ⁴⁷Università di Milano, Dipartimento di Fisica and INFN, I-20133 Milano, Italy
- ⁴⁸University of Mississippi, University, Mississippi 38677, USA
- ⁴⁹Université de Montréal, Physique des Particules, Montréal, Québec, Canada H3C 3J7
- ⁵⁰Mount Holyoke College, South Hadley, Massachusetts 01075, USA
- ⁵¹Università di Napoli Federico II, Dipartimento di Scienze Fisiche and INFN, I-80126, Napoli, Italy
- ⁵²NIKHEF, National Institute for Nuclear Physics and High Energy Physics, NL-1009 DB Amsterdam, The Netherlands
- ⁵³University of Notre Dame, Notre Dame, Indiana 46556, USA
- ⁵⁴Ohio State University, Columbus, Ohio 43210, USA
- ⁵⁵University of Oregon, Eugene, Oregon 97403, USA
- ⁵⁶Università di Padova, Dipartimento di Fisica and INFN, I-35131 Padova, Italy
- ⁵⁷Laboratoire de Physique Nucléaire et de Hautes Energies, IN2P3/CNRS, Université Pierre et Marie Curie-Paris6, Université Denis Diderot-Paris7, F-75252 Paris, France
- ⁵⁸University of Pennsylvania, Philadelphia, Pennsylvania 19104, USA
- ⁵⁹Università di Perugia, Dipartimento di Fisica and INFN, I-06100 Perugia, Italy
- ⁶⁰Università di Pisa, Dipartimento di Fisica, Scuola Normale Superiore and INFN, I-56127 Pisa, Italy
- ⁶¹Princeton University, Princeton, New Jersey 08544, USA
- ⁶²Università di Roma La Sapienza, Dipartimento di Fisica and INFN, I-00185 Roma, Italy
- ⁶³Universität Rostock, D-18051 Rostock, Germany
- ⁶⁴Rutherford Appleton Laboratory, Chilton, Didcot, Oxon, OX11 0QX, United Kingdom
- ⁶⁵DSM/Dapnia, CEA/Saclay, F-91191 Gif-sur-Yvette, France
- ⁶⁶University of South Carolina, Columbia, South Carolina 29208, USA
- ⁶⁷Stanford Linear Accelerator Center, Stanford, California 94309, USA
- ⁶⁸Stanford University, Stanford, California 94305-4060, USA
- ⁶⁹State University of New York, Albany, New York 12222, USA
- ⁷⁰University of Tennessee, Knoxville, Tennessee 37996, USA
- ⁷¹University of Texas at Austin, Austin, Texas 78712, USA
- ⁷²University of Texas at Dallas, Richardson, Texas 75083, USA
- ⁷³Università di Torino, Dipartimento di Fisica Sperimentale and INFN, I-10125 Torino, Italy
- ⁷⁴Università di Trieste, Dipartimento di Fisica and INFN, I-34127 Trieste, Italy
- ⁷⁵IFIC, Universitat de Valencia-CSIC, E-46071 Valencia, Spain
- ⁷⁶University of Victoria, Victoria, British Columbia, Canada V8W 3P6
- ⁷⁷Department of Physics, University of Warwick, Coventry CV4 7AL, United Kingdom
- ⁷⁸University of Wisconsin, Madison, Wisconsin 53706, USA

(Received 28 April 2008; published 26 February 2009)

We use a sample of 384×10^6 $B\bar{B}$ events collected with the BABAR detector at the PEP-II e^+e^- collider to study angular distributions in the rare decays $B \rightarrow K^*\ell^+\ell^-$, where $\ell^+\ell^-$ is either e^+e^- or $\mu^+\mu^-$. For low dilepton invariant masses, $m_{\ell\ell} < 2.5$ GeV/ c^2 , we measure a lepton forward-backward asymmetry $\mathcal{A}_{\text{FB}} = 0.24^{+0.18}_{-0.23} \pm 0.05$ and K^* longitudinal polarization $F_L = 0.35 \pm 0.16 \pm 0.04$. For $m_{\ell\ell} > 3.2$ GeV/ c^2 , we measure $\mathcal{A}_{\text{FB}} = 0.76^{+0.52}_{-0.32} \pm 0.07$ and $F_L = 0.71^{+0.20}_{-0.22} \pm 0.04$.

DOI: 10.1103/PhysRevD.79.031102

PACS numbers: 13.20.He

*Deceased.

†Now at Temple University, Philadelphia, Pennsylvania 19122, USA.

‡Now at Tel Aviv University, Tel Aviv, 69978, Israel.

§Also with Università di Perugia, Dipartimento di Fisica, Perugia, Italy.

||Also with Università di Sassari, Sassari, Italy.

B. AUBERT *et al.*

The decays $B \rightarrow K^* \ell^+ \ell^-$, where $K^* \rightarrow K\pi$ and $\ell^+ \ell^-$ is either an $e^+ e^-$ or $\mu^+ \mu^-$ pair, arise from flavor-changing neutral currents (FCNC), which are forbidden at tree level in the standard model (SM). The lowest-order SM processes contributing to these decays are the photon or Z penguin and the $W^+ W^-$ box diagrams shown in Fig. 1. The amplitudes can be expressed in terms of effective Wilson coefficients for the electromagnetic penguin, C_7^{eff} , and the vector and axial-vector electroweak contributions, C_9^{eff} and C_{10}^{eff} , respectively, arising from the interference of the Z penguin and $W^+ W^-$ box diagrams [1]. The angular distributions in these decays as a function of dilepton mass squared $q^2 = m_{\ell^+ \ell^-}^2$ are sensitive to many possible new physics contributions [2].

We describe measurements of the distribution of the angle θ_K between the K and the B directions in the K^* rest frame. A fit to $\cos\theta_K$ of the form [3]

$$\frac{3}{2} F_L \cos^2 \theta_K + \frac{3}{4} (1 - F_L) (1 - \cos^2 \theta_K) \quad (1)$$

determines F_L , the K^* longitudinal polarization fraction. We also describe measurements of the distribution of the angle θ_ℓ between the ℓ^+ (ℓ^-) and the B (\bar{B}) direction in the $\ell^+ \ell^-$ rest frame. A fit to $\cos\theta_\ell$ of the form [3]

$$\frac{3}{4} F_L (1 - \cos^2 \theta_\ell) + \frac{3}{8} (1 - F_L) (1 + \cos^2 \theta_\ell) + \mathcal{A}_{\text{FB}} \cos \theta_\ell \quad (2)$$

determines \mathcal{A}_{FB} , the lepton forward-backward asymmetry. These measurements are done in a low q^2 region $0.1 < q^2 < 6.25 \text{ GeV}^2/c^4$, and in a high q^2 region above $10.24 \text{ GeV}^2/c^4$. We remove the J/ψ and $\psi(2S)$ resonances by vetoing events in the regions $q^2 = 6.25\text{--}10.24 \text{ GeV}^2/c^4$ and $q^2 = 12.96\text{--}14.06 \text{ GeV}^2/c^4$ respectively.

The SM predicts a distinctive variation of \mathcal{A}_{FB} arising from the interference between the different amplitudes. The expected SM dependence of \mathcal{A}_{FB} and F_L on q^2 along with variations due to opposite-sign Wilson coefficients are shown in Fig. 3. At low q^2 , where C_7^{eff} dominates, \mathcal{A}_{FB} is expected to be small with a zero-crossing point at $q^2 \sim 4 \text{ GeV}^2/c^4$ [4–6]. There is an experimental constraint on the magnitude of C_7^{eff} coming from the branching fraction for $b \rightarrow s\gamma$ [6,7], which corresponds to the limit $q^2 \rightarrow 0$. However, a reversal of the sign of C_7^{eff} is allowed. At high

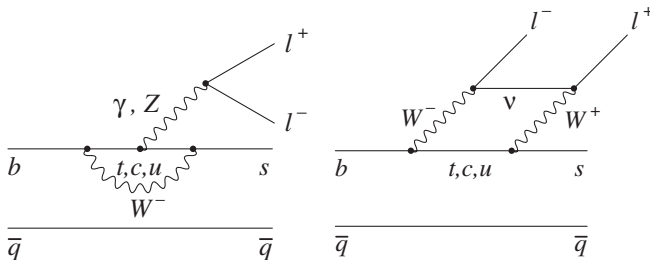


FIG. 1. Lowest-order Feynman diagrams for $b \rightarrow s \ell^+ \ell^-$.

q^2 , the product of C_9^{eff} and C_{10}^{eff} is expected to give a large positive asymmetry. Right-handed weak currents have an opposite-sign $C_9^{\text{eff}} C_{10}^{\text{eff}}$ which would give a negative \mathcal{A}_{FB} at high q^2 . Contributions from non-SM processes can change the magnitudes and relative signs of C_7^{eff} , C_9^{eff} and C_{10}^{eff} , and may introduce complex phases between them [3,8]. An experimental determination of F_L is required to obtain a model-independent \mathcal{A}_{FB} result, and thus avoid drawing possibly incorrect inferences about new physics from our observations.

We reconstruct signal events in six separate flavor-specific final states containing an $e^+ e^-$ or $\mu^+ \mu^-$ pair, and a $K^*(892)$ candidate reconstructed as $K^+ \pi^-$, $K^+ \pi^0$ or $K_S^0 \pi^+$ (or their charge conjugates). To understand combinatorial backgrounds we also reconstruct samples containing the same hadronic final states and $e^\pm \mu^\mp$ pairs, where no signal is expected because of lepton-flavor conservation. To understand backgrounds from hadrons (h) misidentified as muons, we similarly reconstruct samples containing $h^\pm \mu^\mp$ pairs with no particle identification requirement for the h^\pm .

We use a data set of $384 \times 10^6 B\bar{B}$ pairs collected at the $\Upsilon(4S)$ resonance with the BABAR detector [9] at the PEP-II asymmetric-energy $e^+ e^-$ collider. Tracking is provided by a five-layer silicon vertex tracker and a 40-layer drift chamber in a 1.5 T magnetic field. We identify electrons with a CsI(Tl) electromagnetic calorimeter, muons with an instrumented magnetic flux return, and K^+ using a detector of internally reflected Cherenkov light as well as ionization energy loss information. Charged tracks other than identified e , μ and K candidates are treated as pions. Electrons (muons) are required to have momenta $p > 0.3(0.7) \text{ GeV}/c$ in the laboratory frame. We add photons to electrons when they are consistent with bremsstrahlung, and do not use electrons that arise from photon conversions to low-mass $e^+ e^-$ pairs. Neutral $K_S^0 \rightarrow \pi^+ \pi^-$ candidates are required to have an invariant mass consistent with the nominal K^0 mass [10], and a flight distance from the $e^+ e^-$ interaction point which is more than 3 times its uncertainty. Neutral pion candidates are formed from two photons with $E_\gamma > 50 \text{ MeV}$, and an invariant mass between 115 and 155 MeV/c^2 . We require $K^*(892)$ candidates to have an invariant mass $0.82 < M(K\pi) < 0.97 \text{ GeV}/c^2$.

$B \rightarrow K^* \ell^+ \ell^-$ decays are characterized by the kinematic variables $m_{\text{ES}} = \sqrt{s/4 - p_B^{*2}}$ and $\Delta E = E_B^* - \sqrt{s}/2$, where p_B^* and E_B^* are the reconstructed B momentum and energy in the center-of-mass (CM) frame, and \sqrt{s} is the total CM energy. We define a fit region $m_{\text{ES}} > 5.2 \text{ GeV}/c^2$, with $-0.07 < \Delta E < 0.04$ ($-0.04 < \Delta E < 0.04$) GeV for $e^+ e^-$ ($\mu^+ \mu^-$) final states in the low q^2 region, and $-0.08 < \Delta E < 0.05$ ($-0.05 < \Delta E < 0.05$) GeV for high q^2 . We use the wider (narrower) ΔE windows to select the $e^\pm \mu^\mp$ ($h^\pm \mu^\mp$) background samples.

The most significant background arises from random combinations of leptons from semileptonic B and D de-

cays. In $B\bar{B}$ events the leptons are kinematically correlated if they come from $B \rightarrow D^{(*)}\ell\nu$, $D \rightarrow K^{(*)}\ell\nu$. Uncorrelated backgrounds combine leptons from separate B decays or from continuum $e^+e^- \rightarrow c\bar{c}$ events. We suppress these types of combinatorial background through the use of neural networks (NN). For each final state we use four separate NN designed to suppress either continuum or $B\bar{B}$ backgrounds in either the low or high q^2 regions, and different selections of NN inputs are used depending on q^2 bin (low, high), the identity of the leptons in the final state (e , μ), and the type of background ($B\bar{B}$, continuum). Inputs include:

- (i) event thrust;
- (ii) ratio of second-to-zeroth Fox-Wolfram moments [11];
- (iii) m_{ES} and ΔE of the rest of the event (ROE), comprising all charged tracks and neutral energy deposits not used to reconstruct the signal candidate;
- (iv) the magnitude of the total event transverse momentum, which is correlated with missing energy due to unreconstructed neutrinos in background semileptonic decays;
- (v) dilepton system's distance of closest approach along the beam axis, and separately in the plane perpendicular to the beam axis, to the primary interaction point;
- (vi) vertex probability of the signal candidate and, separately, of the dilepton system;
- (vii) the cosines in the CM frame of the angle between the B candidate's momentum and the beam axis, the angle between the event thrust axis and the beam axis (θ_{thrust}), the angle between the ROE thrust axis and the beam axis ($\theta_{\text{thrust}}^{\text{ROE}}$), and the angle between $\theta_{\text{thrust}}^{\text{ROE}}$ and θ_{thrust} .

There is also a background contribution in the signal region from $B \rightarrow D(K^*\pi)\pi$ decays, where both pions are misidentified. The misidentification rates for muons and electrons are $\sim 2\%$ and $\sim 0.1\%$, respectively, so this background is only significant in the $\mu^+\mu^-$ final states. These events are vetoed if the invariant mass of the $K^*\pi$ system is in the range 1.84–1.90 GeV/ c^2 .

We optimize the NN and ΔE selections for each final state in each q^2 bin to give the best combined statistical signal significance in the m_{ES} signal region $m_{\text{ES}} > 5.27$ GeV/ c^2 for the sum of all six final states. After all these selections have been applied, the final reconstruction efficiencies and expected yields for signal events (calculated using world average branching fractions [7]), as well as expected yields for background events in the signal region, are shown in Table I.

For each q^2 region, we combine events from all six final states and perform three successive unbinned maximum likelihood fits. Because of the relatively small number of signal candidates in each q^2 region, a simultaneous fit over m_{ES} , $\cos\theta_K$, and $\cos\theta_\ell$ is unlikely to converge and a

TABLE I. Signal efficiencies (%), and expected signal and background yields for $m_{\text{ES}} > 5.27$ GeV/ c^2 , for low and high q^2 regions.

Mode	Signal Eff.		Signal Yield		Bkgd. Yield	
	low	high	low	high	low	high
$K^+\pi^0\mu^+\mu^-$	1.6	3.1	1.0	1.8	0.7	3.8
$K_S^0\pi^+\mu^+\mu^-$	3.6	5.5	3.0	4.5	0.3	1.4
$K^+\pi^-\mu^+\mu^-$	4.5	8.1	5.5	9.6	0.0	3.1
$K^+\pi^0e^+e^-$	4.6	5.3	2.8	3.1	1.7	2.4
$K_S^0\pi^+e^+e^-$	7.0	5.4	5.9	4.4	0.3	1.4
$K^+\pi^-e^+e^-$	8.6	10.3	10.5	12.2	1.7	2.4
Total Yield			28.6	35.8	4.8	14.5

sequential fitting procedure is required. We initially fit the m_{ES} distribution using events with $m_{\text{ES}} > 5.2$ GeV/ c^2 to obtain the signal and background yields, N_S and N_B , respectively. We use an ARGUS shape [12] with a free shape parameter to describe the combinatorial background in this fit. For the signal, we use a Gaussian shape with a mean $m_{\text{ES}} = 5.2791 \pm 0.0001$ GeV/ c^2 and $\sigma = 2.60 \pm 0.03$ MeV/ c^2 , which are determined from a fit to the vetoed charmonium samples. In this and subsequent fits we account for a small contribution from misidentified hadrons by subtracting the $K^*h^\pm\mu^\mp$ events, weighted by the probability for the h^\pm to be misidentified as a muon. We also account in all fits for charmonium events that escape the veto, and for misreconstructed signal events. We estimate contributions from nonresonant $K\pi$ decays by fitting events outside the K^* mass window in the range 0.7–1.1 GeV/ c^2 . We find no signal-like events that are not accounted for by the tails of the resonant mass distribution, and thus do not expect any significant contribution from nonresonant events within the mass window.

The second fit is to the cosine of the helicity angle of the K^* decay, $\cos\theta_K$, for events with $m_{\text{ES}} > 5.27$ GeV/ c^2 . In this fit, the only free parameter is F_L , with the normalizations for signal and combinatorial background events taken from the initial m_{ES} fit. The background normalization is obtained by integrating, for $m_{\text{ES}} > 5.27$ GeV/ c^2 , the ARGUS shape resulting from the m_{ES} fit. We model the $\cos\theta_K$ shape of the combinatorial background using e^+e^- and $\mu^+\mu^-$ events, as well as lepton-flavor violating $e^+\mu^-$ and μ^+e^- events, in the $5.20 < m_{\text{ES}} < 5.27$ GeV/ c^2 sideband. The signal distribution given in Eq. (1) is folded with the detector acceptance as a function of $\cos\theta_K$, which is obtained from simulated signal events.

The final fit is to the cosine of the lepton helicity angle, $\cos\theta_\ell$, for events with $m_{\text{ES}} > 5.27$ GeV/ c^2 . The only free parameter in this fit is \mathcal{A}_{FB} , with the signal distribution given in Eq. (2) folded with the detector acceptance as a function of $\cos\theta_\ell$. In this fit, the value of F_L is fixed from the result of the second fit, and normalizations for signal and combinatorial background events are identical to those used in the second fit. We constrain the $\cos\theta_\ell$ shape of the

B. AUBERT *et al.*

 TABLE II. Results for the $B \rightarrow J/\psi K^*$ control samples. ΔBF are the differences between the measured branching fractions and the world average value [10]. The previously measured $F_L = 0.56 \pm 0.01$ [13], and the expected $\mathcal{A}_{\text{FB}} = 0$.

Mode	$\Delta\text{BF} (10^{-3})$	F_L	\mathcal{A}_{FB}
$K^+ \pi^0 \mu^+ \mu^-$	$+0.09 \pm 0.12$	0.54 ± 0.03	-0.04 ± 0.05
$K_S^0 \pi^+ \mu^+ \mu^-$	$+0.02 \pm 0.11$	0.55 ± 0.02	$+0.00 \pm 0.05$
$K^+ \pi^- \mu^+ \mu^-$	-0.03 ± 0.07	0.56 ± 0.02	-0.02 ± 0.02
$K^+ \pi^0 e^+ e^-$	$+0.16 \pm 0.10$	0.54 ± 0.03	$+0.02 \pm 0.03$
$K_S^0 \pi^+ e^+ e^-$	$+0.07 \pm 0.10$	0.55 ± 0.02	-0.02 ± 0.04
$K^+ \pi^- e^+ e^-$	$+0.02 \pm 0.07$	0.56 ± 0.02	$+0.01 \pm 0.02$

combinatorial background using the same sideband samples as for the $\cos\theta_K$ fit. The correlated leptons from $B \rightarrow D^{(*)} \ell \nu$, $D \rightarrow K^{(*)} \ell \nu$ give rise to an m_{ES} -dependent peak in the combinatorial background at $\cos\theta_\ell > 0.7$, and we consider this correlation in our study of systematic errors. No such correlation is observed for $\cos\theta_K$.

We test our fits using the large sample of vetoed charmonium events. The branching fractions (BF) and K^* polarization for $B \rightarrow J/\psi K^*$ are well known [10,13], and \mathcal{A}_{FB} is expected to be zero. The results of the fits to the six final states are all consistent with expected values (see Table II). We further test our methodology by performing the m_{ES} and $\cos\theta_\ell$ fits on a sample of $B^+ \rightarrow K^+ \ell^+ \ell^-$ decays. The results are given in Table III and are consistent with negligible forward-backward asymmetry, as expected in the SM and most new physics models [14].

We validate the fit model by performing ensembles of fits to datasets with events drawn from simulated signal and background event samples. The input SM values of F_L and \mathcal{A}_{FB} are reproduced with the expected statistical errors. A few percent of the fits do not converge due to small signal yields. We have also performed fits using signal events generated with widely varying values of C_7^{eff} , C_9^{eff} , and C_{10}^{eff} covering the physically allowed regions of F_L and \mathcal{A}_{FB} , and find minimal bias in our fits.

The systematic errors on the fitted values of F_L and \mathcal{A}_{FB} are summarized in Table IV. The uncertainties in the fitted signal yields N_S , due to variations in the ARGUS shape in the m_{ES} fits, are propagated into the angular fits. The errors on the fitted F_L values are propagated into the \mathcal{A}_{FB} fits. We vary the combinatorial background shapes by dividing

 TABLE III. Results for the fits to the $K\ell^+\ell^-$ and $K^*\ell^+\ell^-$ samples. N_S is the number of signal events in the m_{ES} fit. The quoted errors are statistical only.

Decay	q^2	N_S	F_L	\mathcal{A}_{FB}
$K\ell^+\ell^-$	low	26.0 ± 5.7		$+0.04^{+0.16}_{-0.24}$
	high	26.5 ± 6.7		$+0.20^{+0.14}_{-0.22}$
$K^*\ell^+\ell^-$	low	27.2 ± 6.3	0.35 ± 0.16	$+0.24^{+0.18}_{-0.23}$
	high	36.6 ± 9.6	$0.71^{+0.20}_{-0.22}$	$+0.76^{+0.52}_{-0.32}$

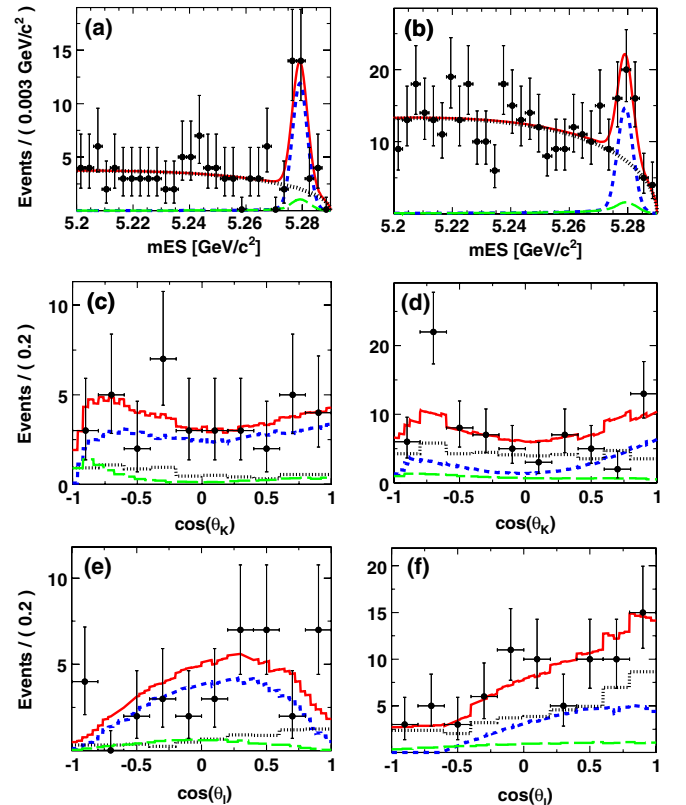
 PHYSICAL REVIEW D **79**, 031102(R) (2009)

 TABLE IV. Systematic errors on the measurements of F_L and \mathcal{A}_{FB} in the $K^*\ell^+\ell^-$ samples.

Source of error	F_L		\mathcal{A}_{FB}	
	low q^2	high q^2	low q^2	high q^2
m_{ES} fit yields	0.001	0.016	0.003	0.002
F_L fit error			0.025	0.022
Background shape	0.011	0.008	0.017	0.021
Signal model	0.036	0.034	0.030	0.038
Fit bias	0.012	0.020	0.023	0.052
Misreconstructed signal	0.010	0.010	0.020	0.020
Total	0.041	0.044	0.052	0.074

the sideband sample into two disjoint regions in m_{ES} . We vary the signal model using simulated events generated with different form factors [5,15], and with a range of values of C_7^{eff} , C_9^{eff} , and C_{10}^{eff} , to determine an average fit bias. Finally, the modeling of misreconstructed signal events is constrained by the fits to the charmonium samples (Table II), where it is the largest systematic uncertainty.

The final fits to the $K^*\ell^+\ell^-$ samples are shown in Fig. 2. The results for F_L and \mathcal{A}_{FB} are given in Table III and are shown in Fig. 3. In the low q^2 region, where we expect


 FIG. 2 (color online). $K^*\ell^+\ell^-$ fits: (a) low q^2 m_{ES} , (b) high q^2 m_{ES} , (c) low q^2 $\cos\theta_K$, (d) high q^2 $\cos\theta_K$, (e) low q^2 $\cos\theta_\ell$, (f) high q^2 $\cos\theta_\ell$; with combinatorial (dotted line) and peaking (long dashed line) background, signal (short dashed line) and total (solid line) fit distributions superimposed on the data points.

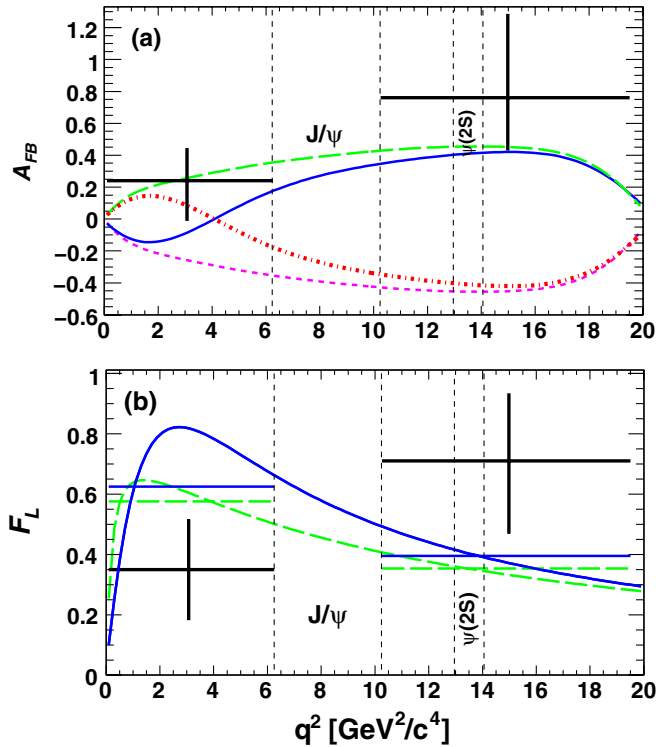


FIG. 3 (color online). Plots of our results for (a) \mathcal{A}_{FB} and (b) F_L for the decay $B \rightarrow K^* \ell^+ \ell^-$ showing comparisons with SM (solid line); $C_7^{\text{eff}} = -C_7^{\text{eff}}$ (long dashed line); $C_9^{\text{eff}} C_{10}^{\text{eff}} = -C_9^{\text{eff}} C_{10}^{\text{eff}}$ (short dashed line); $C_7^{\text{eff}} = -C_7^{\text{eff}}$, $C_9^{\text{eff}} C_{10}^{\text{eff}} = -C_9^{\text{eff}} C_{10}^{\text{eff}}$ (dash-dotted line). Statistical and systematic errors are added in quadrature. Expected F_L values integrated over each q^2 region are also shown. The F_L curves with $C_9^{\text{eff}} C_{10}^{\text{eff}} = -C_9^{\text{eff}} C_{10}^{\text{eff}}$ are nearly identical to the two curves shown.

$\mathcal{A}_{\text{FB}} \sim -0.03$ and $F_L \sim 0.63$ from the SM, we measure $\mathcal{A}_{\text{FB}} = 0.24_{-0.23}^{+0.18} \pm 0.05$ and $F_L = 0.35 \pm 0.16 \pm 0.04$, where the first error is statistical and the second is systematic. In the high q^2 region, the SM expectation is $\mathcal{A}_{\text{FB}} \sim 0.38$ and $F_L \sim 0.40$, and we measure $\mathcal{A}_{\text{FB}} = 0.76_{-0.32}^{+0.52} \pm$

0.07 and $F_L = 0.71_{-0.22}^{+0.20} \pm 0.04$, with a signal yield of 36.6 ± 9.6 events. Theoretical uncertainties on the expected SM F_L and \mathcal{A}_{FB} values are generally difficult to characterize in the high q^2 region, and although under better control for $1 < q^2 < 6 \text{ GeV}^2/c^4$, the extension of our low q^2 region below $1 \text{ GeV}^2/c^4$ makes estimates of uncertainties there difficult also. The quoted values are obtained using our implementation of the physics models described in [4,15], corresponding to the SM curves in Fig. 3.

The expected SM value of C_{10}^{eff} at next-to-next-to-leading logarithmic (NNLL) order is $C_{10}^{\text{eff}} = -4.43$ [16]. A more recent NNLL calculation which evaluates contributions from the full set of seven form factors gives $C_{10}^{\text{eff}} = -4.13$ [17]. The magnitude of possible contributions from new physics to C_{10} can be constrained if $\mathcal{A}_{\text{FB}} > 0$ at high q^2 . By combining such a constraint on \mathcal{A}_{FB} with inclusive $b \rightarrow s \ell^+ \ell^-$ branching fraction results, an upper bound of $|C_{10}^{\text{NP}}| \leq 7$ can be obtained, improving on an upper bound derived solely from branching fraction results of $|C_{10}^{\text{NP}}| \leq 10$ [18]. Our results are consistent with measurements by Belle [19], and replace the earlier BABAR results in which only a lower limit on \mathcal{A}_{FB} was set in the low q^2 region [20].

We are grateful for the excellent luminosity and machine conditions provided by our PEP-II colleagues, and for the substantial dedicated effort from the computing organizations that support BABAR. The collaborating institutions wish to thank SLAC for its support and kind hospitality. This work is supported by DOE and NSF (USA), NSERC (Canada), CEA and CNRS-IN2P3 (France), BMBF and DFG (Germany), INFN (Italy), FOM (The Netherlands), NFR (Norway), MES (Russia), MEC (Spain), and STFC (United Kingdom). Individuals have received support from the Marie Curie EIF (European Union) and the A. P. Sloan Foundation.

- [1] G. Buchalla, A. J. Buras, and M. E. Lautenbacher, Rev. Mod. Phys. **68**, 1125 (1996).
- [2] G. Burdman, Phys. Rev. D **52**, 6400 (1995); J. L. Hewett and J. D. Wells, Phys. Rev. D **55**, 5549 (1997); T. Feldmann and J. Matias, J. High Energy Phys. 01 (2003) 074; W. J. Li, Y. B. Dai, and C. S. Huang, Eur. Phys. J. C **40**, 565 (2005); Y. G. Xu, R. M. Wang, and Y. D. Yang, Phys. Rev. D **74**, 114019 (2006); P. Colangelo, F. De Fazio, R. Ferrandes, and T. N. Pham, Phys. Rev. D **73**, 115006 (2006).
- [3] F. Kruger and J. Matias, Phys. Rev. D **71**, 094009 (2005).
- [4] A. Ali, P. Ball, L. T. Handoko, and G. Hiller, Phys. Rev. D **61**, 074024 (2000).
- [5] F. Kruger, L. M. Sehgal, N. Sinha, and R. Sinha, Phys. Rev. D **61**, 114028 (2000); **63**, 019901(E) (2001); A. Ali, E. Lunghi, C. Greub, and G. Hiller, Phys. Rev. D **66**, 034002 (2002); K. S. M. Lee, Z. Ligeti, I. W. Stewart, and F. J. Tackmann, Phys. Rev. D **75**, 034016 (2007).
- [6] M. Beneke, T. Feldmann, and D. Seidel, Nucl. Phys. **B612**, 25 (2001).
- [7] E. Barberio *et al.* (Heavy Flavor Averaging Group (HFAG) Collaboration), arXiv:0704.3575; C. Bobeth, M. Bona, A. J. Buras, T. Ewerth, M. Pierini, L. Silvestrini, and A. Weiler, Nucl. Phys. **B726**, 252 (2005).
- [8] A. Hovhannisyann, W. S. Hou, and N. Mahajan, Phys. Rev. D **77**, 014016 (2008).
- [9] B. Aubert *et al.* (BABAR Collaboration), Nucl. Instrum. Methods Phys. Res., Sect. A **479**, 1 (2002).

B. AUBERT *et al.*

PHYSICAL REVIEW D **79**, 031102(R) (2009)

- [10] W.M. Yao *et al.* (Particle Data Group), J. Phys. G **33**, 1 (2006).
- [11] G.C. Fox and S. Wolfram, Nucl. Phys. **B149**, 413 (1979); **B157**, 543(E) (1979).
- [12] H. Albrecht *et al.* (ARGUS Collaboration), Z. Phys. C **48**, 543 (1990).
- [13] B. Aubert *et al.* (BABAR Collaboration), Phys. Rev. D **76**, 031102 (2007).
- [14] C. Bobeth, G. Hiller, and G. Piranishvili, J. High Energy Phys. 12 (2007) 040.
- [15] P. Ball and R. Zwicky, Phys. Rev. D **71**, 014029 (2005).
- [16] M. Beneke, T. Feldmann, and D. Seidel, Eur. Phys. J. C **41**, 173 (2005).
- [17] W. Altmannshofer, P. Ball, A. Bharucha, A.J. Buras, D.M. Straub, and M. Wick, J. High Energy Phys. 01 (2009) 019.
- [18] C. Bobeth, G. Hiller, and G. Piranishvili, J. High Energy Phys. 07 (2008) 106.
- [19] A. Ishikawa *et al.*, Phys. Rev. Lett. **96**, 251801 (2006).
- [20] B. Aubert *et al.* (BABAR Collaboration), Phys. Rev. D **73**, 092001 (2006).